

PERIDYNAMICS WITH ADAPTIVE GRID REFINEMENT

DANIELE DIPASQUALE^{*†}, GIULIA SAREGO^{*†}, MIRCO ZACCARIOTTO^{*†} AND
UGO GALVANETTO^{*†}

^{*} Department of Industrial Engineering
University of Padova, Via Venezia 1, Padova 35131, Italy

[†] Centre of Studies and Activities for Space
CISAS - "G.Colombo", Via Venezia 15, Padova 35131, Italy

Key Words: *Peridynamics, Adaptive grid refinement, Multiscale model, Dynamic fracture.*

Abstract. *In recent years, a new non-local theory of continuum mechanics called Peridynamics has proven to be an efficient framework for computational applications to analyze phenomena involving crack formation and propagation in structural materials. In general, fracture mechanics phenomena are linked to a scale length which is comparable to some microscopic structure of the material and this length can be assumed as the maximum distance at which the non-local interaction is still present, that is the so called horizon. The peridynamic numerical implementation of uniform grid spacing with constant horizon for the entire structure does not allow an efficient use of the computational resources. A promising alternative approach is to implement an adaptive grid refinement technique in order to automatically increase the nodal density and decrease the horizon length in the areas in which cracks form and propagate. The numerical solution of the peridynamic theory shows that three different types of convergence can be identified depending on how the ratio between horizon and grid spacing is changed and whether one of the two quantities is kept constant. The adaptive grid refinement is applied in order to analyze how these kinds of convergence influence crack propagation. This analysis is carried out at a local level, since the convergence criterion is employed for a limited area around cracks, while some previous studies applied it on the entire body. The dynamic analysis show phenomena of distortion and spurious reflections of stress waves which pass through the interface regions: for this reason, the effects of non-uniform grid spacing on the propagation of a plane wave are analyzed within a multiscale approach.*

1 INTRODUCTION

The study of brittle fracture dynamics through numerical tools and theories has been drawing more and more interest thanks to its importance for engineering purposes but also for the complexity of the phenomenon itself [1]. Numerical methods based on the classical theory of mechanics, such as XFEM (eXtended Finite Element Method) [2], need additional set of equations in order to overcome the impossibility of defining motion equations, expressed through a differential operator, whenever a discontinuity occurs in the domain. This approach deals with fracture phenomena from a macroscopic point of view thanks to several criteria proposed ad hoc for specific fracture problems in order to properly consider crack occurrence and phenomena such as crack branching. Nevertheless, such criteria have a considerable computational cost and seem not to be able to reproduce all possible phenomena, such as, for example the interaction among different cracks, especially in three dimensional analyses. On the other hand interface elements, often coupled with Cohesive Zone Models (CZM) [3], can only be applied if the path of the crack is known a priori and moreover it is limited by the element discretization. Other numerical methods based on discrete non local theories, such as the atomistic approach [4], deal with fracture dynamics from a microscopic point of view: cracks are due to the break of atomic cohesion forces. However their use is limited from an applicative point of view, due to low computational efficiency. This problem has led to the development of concurrent multiscale models [5], which require complex strategies in order to couple different theories; besides, the atomistic approach has to be applied where the crack nucleation is likely to occur, a region that has to be known a priori. Such limitations have led to the development of a new nonlocal theory of continuum called Peridynamics [6], which seems to be able to accurately treat phenomena of damage and fracture at different spatial length scales [7]. The theory can be equipped as well with a fatigue damage constitutive model in order to study the fatigue crack path evolution [8, 9]. Some authors [10, 11] have proposed to apply the adaptive grid refinement to peridynamic models, decreasing the grid spacing of the discretized domain and the length scale of the nonlocal interaction in the regions characterized by high strain gradient such as those near a crack tip. This is useful in order to improve computational efficiency, maintaining the same accuracy for the solution, and to implement a concurrent multiscale model within a unique mathematical framework. In this study, an adaptive grid refinement technique is applied in order to show its flexibility and efficiency in reproducing phenomena such as crack branching in a homogeneous elastic material in two-dimensional analyses; the set of simulations aims to evaluate how the different types of convergence in the numerical solution of peridynamic theory [10] influence the morphology of the crack propagation. The activation of refinement in proximity of the crack during its propagation is based on an energy trigger, as proposed in literature [11]. The effects due to a non-uniform mesh on elastic wave propagation have been known for a long time in finite element analysis [12], such as spurious reflections, as it can be seen in the studies concerning mono-dimensional peridynamic solutions [10]. In order to conduct the same type of analysis for two-dimensional models, in this paper are evaluated the spurious reflections and distortions of the energy flux due to a continuum wave which propagates in a

model with a non-uniform/multiscale grid for different combinations of reduction in grid spacing and nonlocal interaction.

1.1 Overview of the peridynamic theory

Consider a continuum domain R_0 , the peridynamic theory defines the motion equation of the i^{th} material point located at \mathbf{x}_i (initial position) through the following expression:

$$\rho \ddot{\mathbf{u}}_i = \int_{H_{x_i}} \mathbf{f}(\mathbf{u}(\mathbf{x}, t) - \mathbf{u}(\mathbf{x}_i, t), \mathbf{x} - \mathbf{x}_i) dV_x + \mathbf{b}_i, \quad H_{x_i} = \{\mathbf{x} \in R_0: |\mathbf{x}_i - \mathbf{x}| < \delta\} \quad (1)$$

where \mathbf{u} is the displacement vector field, ρ is the mass density, \mathbf{b} is the external force density, \mathbf{f} is the PairWise force function (PW) which expresses the vector force of the interaction that the material point located at \mathbf{x} exerts on the material point located at \mathbf{x}_i and δ is the horizon, namely the upper limit distance of the interaction between two material points. Eq.1 is the mathematical formulation of the Bond-Based Peridynamics (BBP), which is a particular case of the general formulation called State-Based Peridynamics, see [6] for the limitations of the BBP. The PW force function depends on the constitutive model of the specific material; for a linear elastic material the constitutive model PMB (Prototype Microelastic Brittle) is defined based on the existence of a micropotential function w which is expressed as:

$$w(\boldsymbol{\eta}, \boldsymbol{\xi}) = \frac{cs^2 \|\boldsymbol{\xi}\|}{2} \quad (2)$$

where c is called micromodulus (it is supposed a constant function), $s = \frac{\|\boldsymbol{\xi} + \boldsymbol{\eta}\| - \|\boldsymbol{\xi}\|}{\|\boldsymbol{\xi}\|}$ is the relative elongation, $\boldsymbol{\xi} = \mathbf{x} - \mathbf{x}_i$ is the initial relative position and $\boldsymbol{\eta} = \mathbf{u}(\mathbf{x}, t) - \mathbf{u}(\mathbf{x}_i, t)$ is the current relative displacement; in the BBP the potential energy density $W(\mathbf{x}_i)$ is equal to the integral of the micropotential function (Eq.2) in the horizon sphere centered at \mathbf{x}_i as:

$$W(\mathbf{x}_i) = \frac{1}{2} \int_{H_{x_i}} w(\boldsymbol{\eta}, \boldsymbol{\xi}) dV_x \quad (3)$$

Imposing the equality of the potential energy density expressed in Eq.3 and the potential energy density defined in the classical theory of continuum, the value for the micromodulus in a two-dimensional plane stress analysis is expressed as:

$$c = \frac{6E}{\pi \delta^3 (1 - \nu)} \quad (4)$$

where E is the Young's modulus and ν is the Poisson's ratio. A particular and favorable aspect of Peridynamics is the unambiguous definition of the damage at a material point, based on the definition of the critical relative elongation s_0 . This elongation is related to the material fracture energy G_0 (experimentally measured) through Eq.3; in a plane stress two-dimensional analysis s_0 is calculated as:

$$s_0 = \sqrt{\frac{4\pi G_0}{9E\delta}} \quad (5)$$

So, the PW force function is defined as:

$$\mathbf{f}(\boldsymbol{\eta}, \boldsymbol{\xi}) = \mu(t, \xi) \frac{\partial w(\boldsymbol{\eta}, \boldsymbol{\xi})}{\partial \boldsymbol{\eta}} = \mu(t, \xi)_{CS} \frac{\boldsymbol{\xi} + \boldsymbol{\eta}}{\|\boldsymbol{\xi} + \boldsymbol{\eta}\|} \quad (6)$$

$$\mu(t, \xi) = \begin{cases} 1 & \text{if } s < s_0 \text{ for all } 0 \leq t' \leq t \\ 0 & \text{otherwise} \end{cases}$$

Eqs.6 show a history-dependence of the model, since after a bond breaks, it can't be recovered, the damage is permanent; the damage state to which a material point located at \mathbf{x}_i is subjected is defined as:

$$\varphi(\mathbf{x}_i, t) = 1 - \frac{\int_{H_{x_i}} \mu(\mathbf{x}_i, t, \boldsymbol{\xi}) dV_x}{\int_{H_{x_i}} dV_x} \quad (7)$$

As stated in literature [11], Peridynamics was initially formulated with an implicit assumption of a constant horizon within the whole domain, therefore the change in the horizon from a region to another one requires a proper scaling technique, expressed for the two-dimensional analysis as:

$$w_\varepsilon(\boldsymbol{\eta}, \boldsymbol{\xi}) = \gamma^2 w_\delta(\gamma\boldsymbol{\eta}, \gamma\boldsymbol{\xi}) \quad (8)$$

where $\gamma = \delta/\varepsilon$, in which δ and ε are two different horizon values; the scaling operation is needed in order to maintain constant the strain energy when the domain is subjected to a homogeneous strain, as highlighted in the expression:

$$W_\delta(\mathbf{x}) = \frac{1}{2} \int_{H_\delta} w_\delta(\gamma\boldsymbol{\eta}, \gamma\boldsymbol{\xi}) d(\gamma^2 A) = \frac{1}{2} \int_{H_\varepsilon} \frac{1}{\gamma^2} w_\varepsilon(\boldsymbol{\eta}, \boldsymbol{\xi}) \gamma^2 d(A) = W_\varepsilon(\mathbf{x}) \quad (9)$$

As for what concerns the material points at the interface of two regions with different horizons, the third Newton's law requires that every bond of a specific material point is characterized by a micromodulus (Eq.4) the value of which depends only on the horizon of the material point itself.

2 NUMERICAL IMPLEMENTATION OF ADAPTIVE GRID REFINEMENT

The analyses are carried out with an explicit dynamic solver, in which a mid-point spatial integrator scheme in the discretization of the body is employed [13]. Considering the i^{th} node located at \mathbf{x}_i (called source node), Eq.1 becomes:

$$\rho \ddot{\mathbf{u}}_i^n = \sum_j \mathbf{f}(\mathbf{u}_j^n - \mathbf{u}_i^n, \mathbf{x}_j - \mathbf{x}_i) V_j \beta_j + \mathbf{b}_i^n \quad \forall j \in H_{x_i} \quad (10)$$

where n indicates the temporal step, V_j the volume (which is actually an area for two dimensional analyses) associated to the node located at \mathbf{x}_j (called family node) and β_j is a coefficient employed in order to improve the accuracy of the numerical integration [14]. Eq.10 is implemented and solved through a Velocity-Verlet scheme, thanks to its robustness, reliability and simplicity. The numerical implementation of Peridynamics requires the definition of an adimensional parameter $m=\delta/\Delta x$ (Δx is the grid spacing in X direction); this parameter is fundamental in determining the accuracy and the computational efficiency of the peridynamic solution. Bobaru's studies [10] highlight three types of convergence of the numerical solution of Eq.1 to the theoretical peridynamic and classical theory solution, in particular those which are analyzed in this paper through the application of the adaptive grid refinement are the (δ) convergence and (δm) convergence. As previously mentioned, thanks to the adaptive grid refinement applied to Peridynamics, the chosen convergence is implemented through the decrease of the grid spacing and of the horizon length in the region near the crack whereas in the rest of the model these quantities are not changed in order to reduce the computational cost. In the future will be possible to relate the horizon length to the length scale of the analyzed phenomenon [15], therefore the adaptive grid refinement proposed below allows to make a concurrent multiscale adaptive model. In literature [11], in order to activate the refinement, a trigger based on the strain energy density (Eq.3) is proposed, specifically the initial grid nodes are selected if $W(\mathbf{x}_i) \geq W_t$, where W_t is the threshold value determined by a percentage of the maximum strain energy density within the domain in the considered time step.

The extension of the refined region is determined by the so called visibility criterion [10], which states that the refinement has to be applied to a region of the body which contains all the nodes within a horizon distance from the selected node, as shown in Fig 1. The adopted refinement strategy consists in recursively partitioning the distance between neighboring nodes of an initially uniform grid. The initial spacing is $\Delta x_0 = \Delta y_0$, each subdivision splits in half the spatial interval between nodes, as the following expression states:

$$\Delta x_{level} = \frac{\Delta x_0}{(2^{level})} \quad (11)$$

where $level= 0,1,\dots,i$ identifies the refinement level of the nodes of the grid; a 0 value is associated to the coarsest nodes belonging to the initial grid, as shown in Figure 1; the reduction of the horizon length in the refined portion of the grid depends on the type of the adopted convergence. As shown in Fig 1, an area $V_{level} = \Delta x_{level}^2$ is associated to each node, according to its refinement level; such area is modified for the interface nodes according to the following expressions:

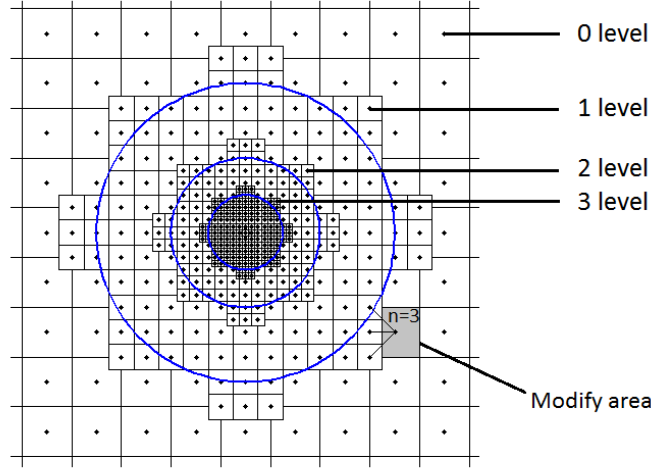


Figure 1: Refinement of the 3rd level for one node identified by the trigger

$$V_{level,int} = \begin{cases} V_{level} - V_{(level+1)}/4 & , \quad n = 1 \\ V_{level} - 3V_{(level+1)}/4 & , \quad n = 2 \\ V_{level} - V_{(level+1)} & , \quad n = 3 \\ V_{level} - 3V_{(level+1)}/2 & , \quad n = 4 \\ V_{level} - 7V_{(level+1)}/4 & , \quad n = 5 \end{cases} \quad (12)$$

where n is the number of nodes of the i^{th} level close to nodes of the lower level (see Fig.1). The refinement process is completed after the upgrading of the new grid bonds and the association of the kinematic quantities obtained by bilinear interpolation.

3 PROPAGATION OF CONTINUUM PLANE WAVE

Fig.1 shows how the developed refinement technique gradually decreases the spatial step. This strategy is in accordance with the studies carried out by Bazant [12] and Bobaru [10], in which spurious reflection phenomena of an elastic wave crossing a region of non-uniform grid step is minimized by adopting a gradual change of grid spacing. The refinement process also includes the reduction of the horizon length in the refined region. The effects on the energy flux due to a non-uniform/multiscale region have to be evaluated. Such evaluation is carried out by taking into account the distortion of the energy flux of a Gauss plane wave when the wave meets along its path a small refined region in a two dimensional plate structure, in which the transverse displacements are blocked, the wave is generated by applying an initial displacement in the x direction:

$$u_0(x, y) = 0.2e^{-\left(\frac{x}{0.03}\right)^2} \quad (13)$$

Figure 2 shows the model plate with the contour plot of the wavefront of total energy density (potential plus kinetic) generated of the initial half wave (it is normalized with respect to half

of its maximum value). The solution is obtained with the use of the linearized equation of Eq.10 [16], the material has Young's modulus $E=1$ and mass density $\rho=1$.

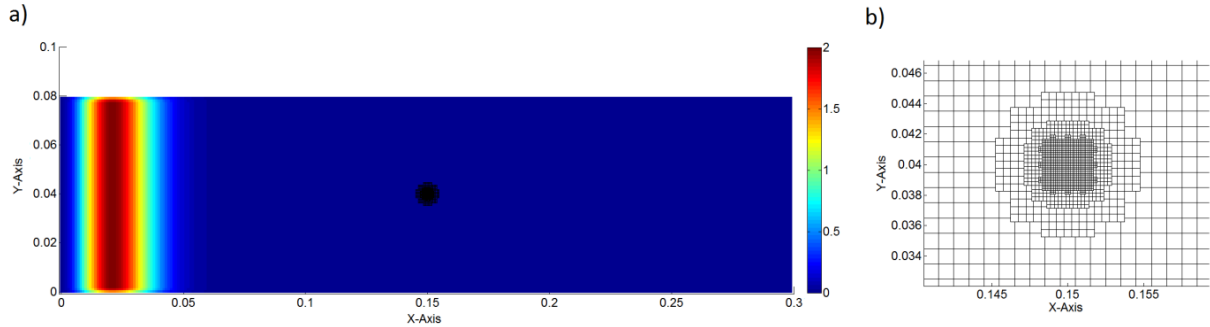


Figure 2: Grid employed for analysis: a) contour plot of total energy density flux, b) example of refined region of 3rd level

Table 1: Characteristic parameters for the models with (δ) convergence, the values in bold correspond to the interface nodes with modified horizon

<i>Level Refinement</i>	$\delta (\times 10^{-3})$	<i>m</i>
0	3.0	3
1	1.5 - 2.1	3 - 4.2
2	0.75 - 1.06	3 - 4.2
3	0.375 - 0.53	3 - 4.2

Table 2: Characteristic parameters for the models with (δm) convergence

<i>Level Refinement</i>	$\delta (\times 10^{-3})$	<i>m</i>
0	3.0	3
1	2.0	4
2	1.25	5
3	0.75	6

Table 1-2 shows the parameters of the implemented models, obtained changing the refinement level and the type of numeric convergence of the refined region; the coarse grid spacing is $\Delta x_0 = 0.001$. As far as the obtained models are concerned adopting the (δ) convergence, some interface nodes show a significant loss of integrating volume in the calculation of Eq.10; in order to minimize such loss the horizon length is increased by an appropriate amount; this strategy drastically reduces the energy flux distortion phenomena, as it is highlighted in the following section.

In Figs 3-4, the longitudinal contours (they are taken at the coordinate $y=0.04$) of the wavefront of the total energy density flux are compared at the moment in which the maximum energy peak is located in the refined region. It is evident how the energy flux is subjected to a

distortion while crossing the refined region; such distortion is more noticeable for those models in which the (δm) convergence is applied.

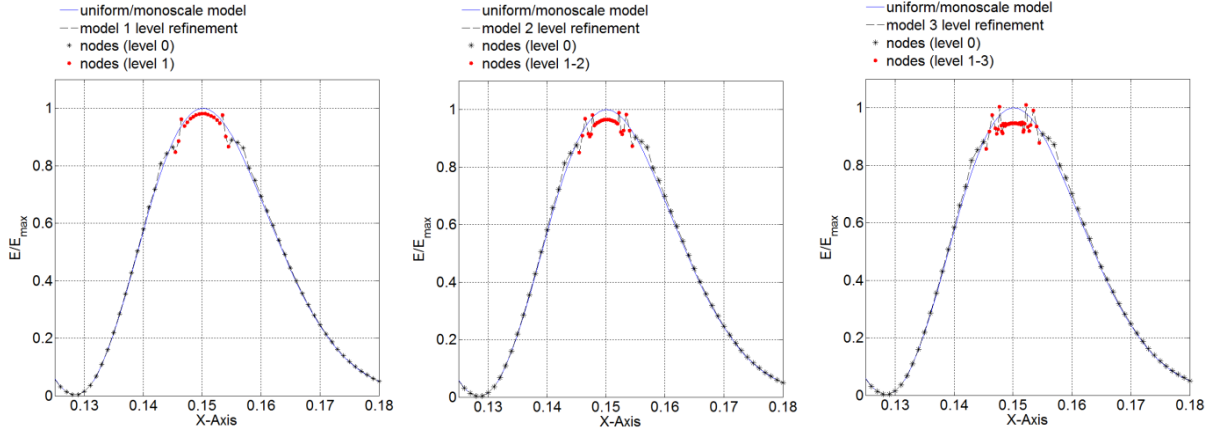


Figure 3: Wavefront of the total energy density for the non-uniform/multiscale models when a (δ) convergence is adopted

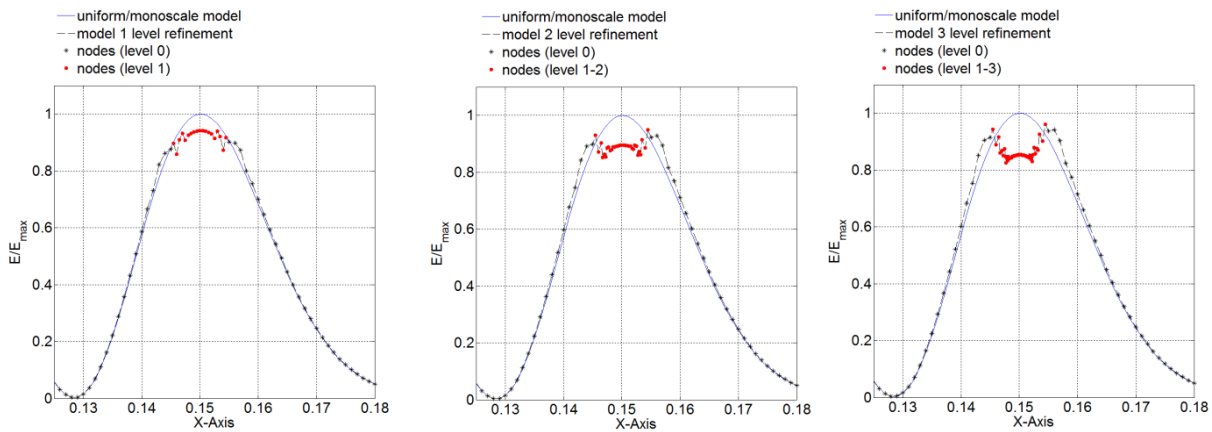


Figure 4: Wavefront of the total energy density for the non-uniform/multiscale models when a (δm) convergence is adopted

To evaluate the distortion, in Table 3 the maximum (ΔE_{max}) and the minimum (ΔE_{min}) percentage variations of the total energy density in the refined region when it is crossed by the energy flux are listed. Such variations are computed with respect to the solution obtained with the uniform/monoscale model; in Figure 5a the energy reduction contours are plotted for one of the analyzed models (which is representative of the behavior of the other models as well). It is highlighted that the interface nodes show a conspicuous energy decrease due to the volume loss in the calculation of Eq.10; this effect can be reduced by modifying the horizon length as it was done for the interface nodes of the (δ) convergence models. In Fig.5b the longitudinal contour of wavefront is plotted for the (δ) convergence model without

modification of the horizon length of interface nodes, these manifest energy reductions of the 37.4%.

Table 3: Total energy density variations of the refined region's nodes and maximum displacement variation of node of coordinates $x = 0.1$, $y = 0.04$

<i>Convergence</i>	<i>Level Refinement</i>	ΔE_{min} [%]	ΔE_{max} [%]	Δu [%]
δ	1	9.83	5.86	0.24
	2	11.00	5.23	0.31
	3	11.63	5.88	0.35
δm	1	17.10	4.38	0.58
	2	18.96	6.25	0.87
	3	20.81	7.27	1.03

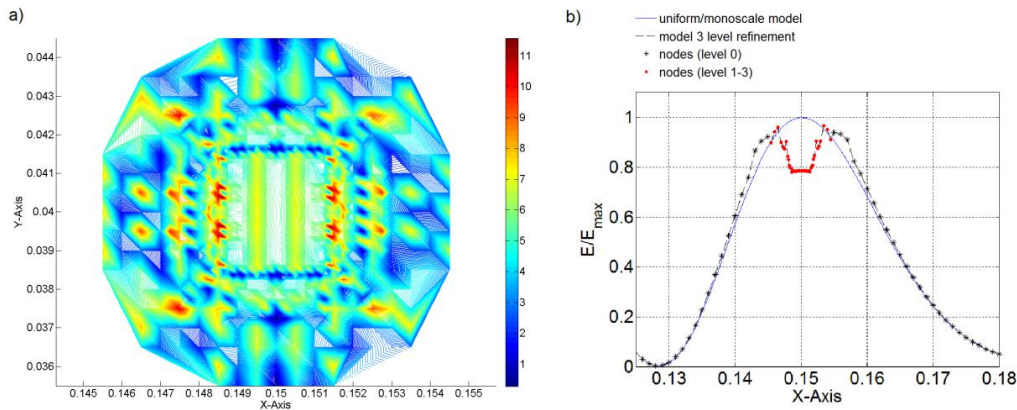


Figure 5: a) Total energy density percentage reduction in the 3rd level refined region within a (δ) convergence model, b) Wavefront's distortion without modification of the horizon length of interface nodes

It is shown that the size of the energy decrease is bigger than the energy increase and that the amount increases as the refinement level goes up. Strategies in order to investigate how to minimize such distortions and how to properly transmit stress waves between regions with different grid spacing and length scale are in progress. This is important since the crack path is determined by the interaction of the stress wave on the crack tip during its propagation. As far as spurious reflections are concerned, the maximum displacement magnitude of the node located at $x=0.1$ and $y=0.04$ is reported in Table 3 (it is expressed as a percentage of the amplitude of the Gaussian wave). The amplitude of the reflected wave increases as the refinement level increases, but this reflection amplitude is of small entity (1% of the Gaussian wave), hence it is negligible.

4 NUMERICAL EXAMPLE

A benchmark test commonly used for verifying a numerical method consists of a pre-notched plate subjected to a uniform traction load on the superior and inferior edges applying

a step load. The load is enough for triggering a crack branching propagation of the crack after an initial phase of self-similar growth. The same case was studied by Belytschko [2] and by Ha [17] which evaluated the effects of the different types of convergence of the numeric solution of BBP on the crack branching morphology. The material is *Soda lime glass* with a Young's modulus $E = 72 \text{ GPa}$, density $\rho = 2440 \text{ kg/m}^3$ and fracture energy $G_0 = 135 \text{ J/m}^2$, the analysis are two-dimensional with plane stress condition. The plate is a $0.10 \times 0.04 \text{ m}^2$ structure with an initial crack of length $0,05 \text{ m}$, the initial discretization is characterized by a grid spacing of $\Delta x_0 = 0.001 \text{ m}$ and horizon $\delta = 0.003 \text{ m}$ ($m=3$), the load to which it is subjected is a tensile step load of 22 MPa .

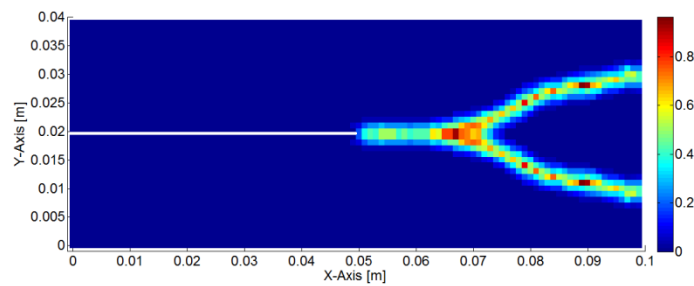


Figure 6: Crack branching at $50\mu\text{s}$ computed with uniform/monoscale model (4000 nodes)

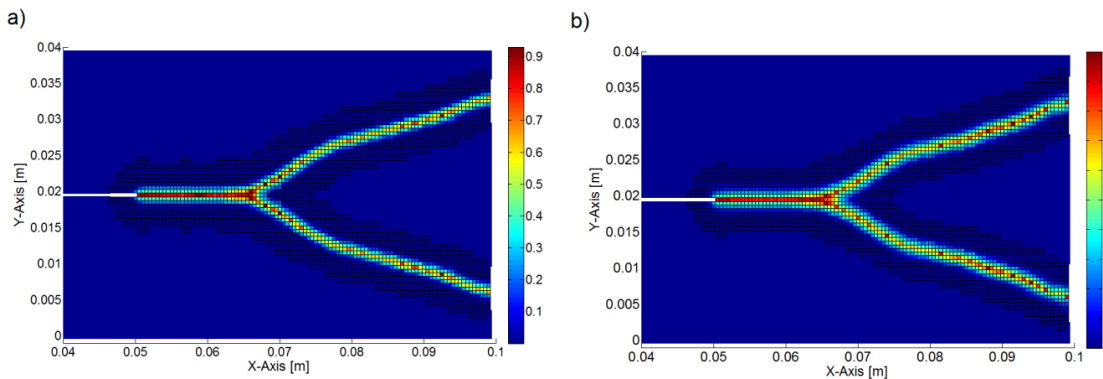


Figure 7: Crack branching at $50\mu\text{s}$ computed with adaptive model: a) refined region with $m=3$ and $\delta=0.0015 \text{ m}$, b) refined region with $m=4$ and $\delta=0.0020 \text{ m}$

The 1st level adaptive grid refinement with different horizon length is applied in order to evaluate the effect of the convergence of the numerical peridynamic solution on the crack morphology. In Figure 6 the results obtained with the initial uniform/monoscale grid model are shown, in Figure 7-8 the crack branching phenomenon obtained applying the adaptive grid refinement. The results show how the horizon length affects the morphology of the crack: as it decreases the slope of the branching increases. We have to consider how the peridynamic theory introduces dispersion relations in the propagation of elastic waves [16]; these depend on the size of the horizon (in addition to those introduced by the numerical discretization). In

an adaptive model each region of the analyzed domain is characterized by a different dispersion relation, further analyses are being carried out to assess the effects of the refinement on the dynamics of the crack propagation.

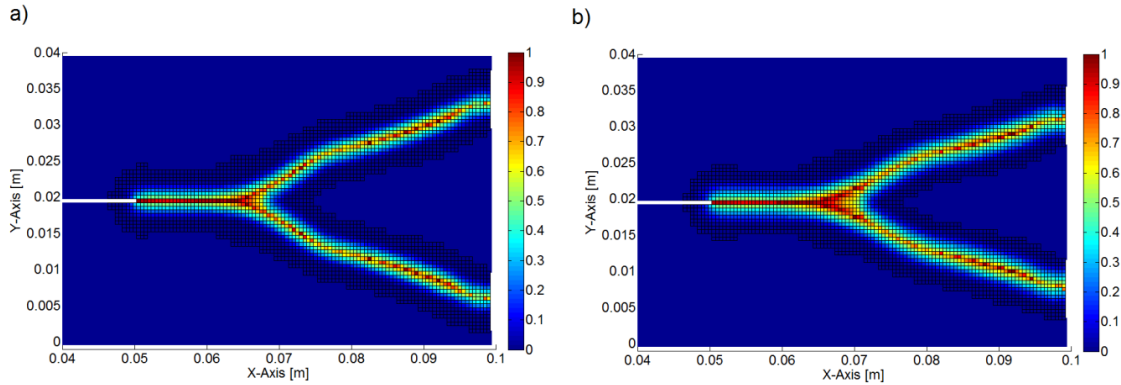


Figure 8: Crack branching at $50\mu s$ computed with adaptive model: a) refined region with $m=5$ and $\delta=0.0025m$, b) refined region with $m=6$ and $\delta=0.003m$

5 CONCLUSIONS

In this study a method to introduce an adaptive grid refinement into a Peridynamic grid has been presented in order to accurately simulate brittle fracture dynamic phenomena such as crack branching. This modelization technique determines an adaptive concurrent multiscale model, in which the grid spacing and the horizon length near the crack during its propagation are reduced. This strategy is fundamental in order to reach a horizon length equal to the length scale of the analyzed phenomenon or of a specific characteristic of the material, starting from initial grid spacing convenient for computational efficiency. Besides, it will be possible to adopt the more convenient discretization for accurately describing the real behavior of the material through a local control of the convergence of the numeric solution. Implementing a non-uniform/multiscale region in the peridynamic solution introduces undesired distortion effects which have been evaluated for different types of convergence of the numeric solution. In particular, the method introduces a reduction of the energy flux which crosses the refined region due to numeric integration errors at the interface nodes, a proposed strategy in this study for minimizing such errors consists in the adoption of a horizon length for those interface nodes which minimize the volume loss in the pairwise force function integral calculation.

REFERENCES

- [1] Ravi-Chandar, K. Dynamic fracture of nominally brittle materials. *International Journal of Fracture* (1998) **90**:83-102.
- [2] Belytschko, T., Chen, H., Xu, J. and Zi, G. Dynamic crack propagation based on loss of hyperbolicity and a new discontinuous enrichment. *International Journal for Numerical*

- Methods in Engineering* (2003) **58**:1873-1905.
- [3] Munoz, J., Galvanetto, U., and Robinson, P. On the numerical simulation of fatigue driven delamination with interface elements. *Int. J. Fatigue* (2006) **28**:1136-1146.
- [4] Zhou, S., Lomdahl, P., Thomson R. and Holian, B.L. Dynamic crack processes via molecular dynamics. *Phys. Rev. Lett.* (1996) **76**:2318–2321.
- [5] Lee, J., Wang, X. and Chen, Y. Multiscale material modeling and its application to a dynamic crack. *Theoretical and Applied Fracture Mechanics* (2009) **51**:33–40.
- [6] Silling, S. and Leouchq, R. Peridynamic Theory of Solid Mechanics. *Advances in Applied Mechanics* (2010) **44**:73-168.
- [7] Askari, E. et al. Peridynamics for multiscale materials modeling,» *Journal of Physics: Conference Series* (2008) **125**.
- [8] Zaccariotto, M. and Galvanetto, U. Modeling of Fatigue Crack Propagation with a Peridynamics Approach. *8th European Solid Mechanics Conference* (2012).
- [9] Zaccariotto, M., Luongo, F., Sarego, G., Dipasquale, D. and Galvanetto, U. Fatigue Crack Propagation with Peridynamics: a sensitivity study of Paris law parameters. *Proceedings of the 4th CEAS Conference Linköping University Electronic Press Linköping* (2013):849-854.
- [10] Bobaru, F., Yabg, M., Alves, L., Silling, S., Askari, E. and Xu, J. Convergence, adaptive refinement, and scaling in 1D peridynamics. *Int. J. Numer Methods Eng.* (2009) **77**:852-877.
- [11] Bobaru, F. and Ha, Y. Adaptive refinement and multiscale modeling in 2D peridynamics. *Journal for Multiscale Computational Engineering* (2011) **9**:635-659.
- [12] Zdeněk, P. and Banžant, Z.C. Spurious reflection of elastic waves due to gradually changing finite element size. *International journal for numerical in engineering* (1983) **19**:631-646.
- [13] Silling S. and Askari, E. A meshfree method based on the peridynamic model of solid mechanics. *Comput. Struct.* (2005) **83**:1526-1535.
- [14] Keping, Y. Enhanced integration method for the peridynamic theory. *Departement of mechanical and Nuclear Engineering* (2011).
- [15] Bobaru, F. and Hu, W. The meaning, selection, an use of the peridynamic horizon and its relation to crack branching in brittle materials. *Int. J Fract.* (2012) **176**:215-222.
- [16] Silling, S. Reformulation of elasticity theory for discontinuities and long-range forces. *Journal of the Mechanics and Physics of Solids* (2000) **48**:175-209.
- [17] Ha, D. and Bobaru, F. Studies of dynamic crack propagation and crack branching with peridynamics. *Int.J. Fract.* (2010) **162**:229-244.